Dynamics of Polyelectrolyte Transport through a Protein Channel as a Function of Applied Voltage

L. Brun,[1] M. Pastoriza-Gallego,[1] G. Oukhaled,[1] J. Mathé,[1] L. Bacri,[1] L. Auvray,[1] and J. Pelta[1,2,*]

[1]*ICMPE, MPI, CNRS-UMR 7182, Université d'Évry, 91025 Évry, France*
[2]*GMCC, Université de Cergy-Pontoise, 2. Avenue A. Chauvin, 95302 Cergy-Pontoise, France*
(Received 7 September 2007; published 17 April 2008)

We study the transport of dextran sulfate through a protein channel as a function of applied voltage. Below 60 mV, the chain's entrance to the pore is hindered by an entropic barrier; above 60 mV, the strong local electric field forces the chain entrance. The effective charge of the polyelectrolyte inside the pore is reduced. We observe two types of blockades which have durations that decrease when the applied voltage increases. The shortest is a straddling time between the polyelectrolyte and the pore; the longest is the translocation time. The translocation time obeys an exponential dependence upon applied voltage.

The first observation of the passage of one single strand DNA through a protein channel, α-hemolysin, in a planar lipid bilayer was observed in 1996 [1]. This pore is asymmetric [2] and stable [3–5]. The sensitivity of techniques for the electrical detection of the molecule translocation through single protein channels has been used in many applications [1,6–9]. These include fundamental studies of confined neutral polymer [10] or charged polymer chains [11,12]. Recent developments include the transformation of nanopores into a manipulation tool and force apparatus by techniques of active control [13,14] and the study of the translocation coupled to the protein unfolding [8].

There is not yet a complete description of the process of polyelectrolyte translocation through a narrow pore but several theories describe the possible phenomena. The blockade rate f is in general described by a Van't Hoff-Arrhenius law: $f = f_0 \exp(|V|/V_0)$ where $f_0 \propto \nu \exp(-U^*/k_B T)$ is the zero voltage event frequency governed by an activation barrier U^* (ν is a frequency factor), and $|V|/V_0 = ze|V|/k_B T$ is a barrier reduction factor due to the applied voltage V, acting on ze, the effective charge of the polyelectrolyte [15]. The barrier U^* is often of entropic origin as is the case for neutral polymer chains, but can be of electrostatic origin because of surface charges, or dielectric effects, or possibly both if some kinds of confinements of the polyelectrolyte counterions are involved. Two alternate theories of charged confined chains predict that the chain's dynamics are dominated by either its mobility or the free-energy barrier. In the first case the translocation time τ is inversely proportional to the applied force, i.e., to the transmembrane voltage [16–19], $\tau \propto 1/V$. In the second case, one expects an exponential dependence on the applied voltage [15], $\tau \propto t_0 \exp(V/V_c)$. Several parameters have been studied, in particular, the influence of the degree of polymerization N and applied voltage on the translocation time and the event frequency. The predictions of the theoretical models [18,20] concerning the influence of the degree of polymer-

ization are confirmed by the experiments [1,12,21,22] and the simulations [23,24]. The behavior depends on the ratio r/L of the polyelectrolyte size over the nanopore length. Experiments show the exponential dependence of the frequency of pore blockades upon applied voltage [8,25,26]. The same behavior is observed at high voltage with a smaller slope [26]. Presently, only a few experiments of the translocation of polyelectrolyte through protein [1,12] or artificial [22,27–29] nanopore have been performed. The translocation time has been found to be inversely proportional to the applied voltage [1,12,27]. A quadratic voltage dependence of the translocation velocity has also been observed [21] in other experiments. Recently, the dynamics of translocation of a polyelectrolyte through a nanopore has been investigated by molecular dynamics using a coarse grained model [24]. The simulations show two different regimes for the probability of translocation as a function of the applied voltage. Both regimes are approximated by an exponential fit. An exponential dependence of the translocation time upon voltage is found below a crossover for which the energy barrier disappears completely in agreement with the experimental data [26]. All-atom molecular dynamics simulation of DNA translocation through synthetic nanopores have also revealed a nonlinear dependence of the DNA translocation velocity on transmembrane bias [30]. Similar results were obtained for RNA translocation through carbon nanotubes [31].

In our experiments, the polyelectrolyte is the dextran sulfate sodium ($M_w = 8$ kDa or $M_w = 500$ kDa) of 31 monomers, each bearing two negative charges. It is added to the *cis* compartment in 1M KCl or 0.1M KCl, 5mM HEPES *p*H 7.4 buffer for a final concentration of 0.5 mg/mL. Experiments on the dynamics of the polyelectrolyte transport were performed by varying the transmembrane voltage V. Lipid bilayers were prepared using a previously described method [1,8]. The channels were inserted by adding 0.30 nmol of monomeric α-hemolysin in the *cis* compartment. The ionic current through one

channel was detected with an Axopatch 200B amplifier. Data are filtered at 10 kHz and acquired at 200 kHz with the DigiData 1322A digitizer coupled with Clampex software (Axon Instruments). The measurements of the transients are based on the statistical analysis of the current traces using IGOR PRO software (WaveMetrics Inc.). Single-channel current traces are obtained between 40 and 155 mV (Fig. 1). A decrease in the applied voltage results in the open pore current decreasing from 165 ± 12 pA down to 41 ± 2.5 pA and we observe a decrease in the event frequency [Figs. 1(a)–1(c)]. Below 40 mV, no events are observed. The mean open pore current is plotted as a function of applied voltage, which indicates a linear behavior and a measured pore conductance, $G = 1069 \pm 15$ pS [Fig. 1(d)], in good agreement with previous experiments [32]. To separate the current blockades caused by dextran sulfate molecules dwelling in the pore from the noisy pore current, a statistical analysis of each current trace is made (see supplementary data in Ref. [33]). The blockade frequency f is plotted as a function of the applied potential (Fig. 2). Two regimes of event frequency are observed. Below 60 mV, the event frequency is strongly sensitive to the applied voltage. Above 60 mV, the behavior is less sensitive and the frequency increases more slowly with the electrical field. Between 60 and 155 mV, the data are well described by an exponential function $f = f_0 \exp(|V|/V_0)$ where $f_0 = 0.5$ Hz, $V_0 = 27.1 \pm 0.03$ mV. The deduced effective charge of the polyelectrolyte is $z = 0.95$ (Fig. 2). This effective charge is determined by several different effects: access resistance [26], charge distribution, and the conformation of the polyelectrolyte at the pore entrance. No theory takes into account all of these contributions. To obtain an estimation of the activation energy (U^*), the frequency factor (ν) is estimated by a barrier penetration calculation [25] to be $\nu \approx 11\,250$ s^{-1} and $U^* \approx 10k_BT$. These values of z and U^* are of the same order of magnitude as the other values found for different charged macromolecules at high ionic strength. For single stranded DNA [25,26] $z = 1.9$ and $U^* \approx 8k_BT$, for protein [8] $z = 0.6$ and $U^* \approx 9k_BT$, or for dextran sulfate [34] at low ionic strength $z = 1.25$ and $U^* \approx 14.5k_BT$.

The regime below 60 mV is very difficult to explore because the probability of blockade is very low. No blockages are observed below 40 mV. This is a clear threshold effect that results from electric driving force not being able to overcome the entropic force necessary to confine the random coil chains inside the pore. If we assume that the electric force and the confinement force [35] are equal at the threshold, we obtain $zeV/L \approx k_BT/r_{\text{pore}}$, and $z \approx (k_BT/eV)(L/r_{\text{pore}})$ leading to $z = 6.2$, close to the bulk value. We have adjusted the variation of the blockade frequency with the potential between 40 and 60 mV with an exponential function as above. The fit yields another estimation of the effective charge and barrier height $z = 5.5$ which is quite close to the estimated bulk charge and $U^* \approx 21k_BT$. This exponential dependence was also predicted by theoretical work [36] in the regime called "reaction limited."

We have analyzed the duration of the current blockades as a function of applied voltage (Fig. 3). Two mean blockade durations are observed, a short and a longer one. They decrease when the applied voltage increases. The dependence of short blockades is well fitted (same χ^2 value) by the two laws described at the beginning of this Letter, associated either to a reciprocal dependence on V or to an exponential dependence. For the longer blockades, we obtain, respectively, for the exponential fit or $1/V$ fit, $\chi^2 = 2.2$ and $\chi^2 = 5.1$. The exponential dependence for
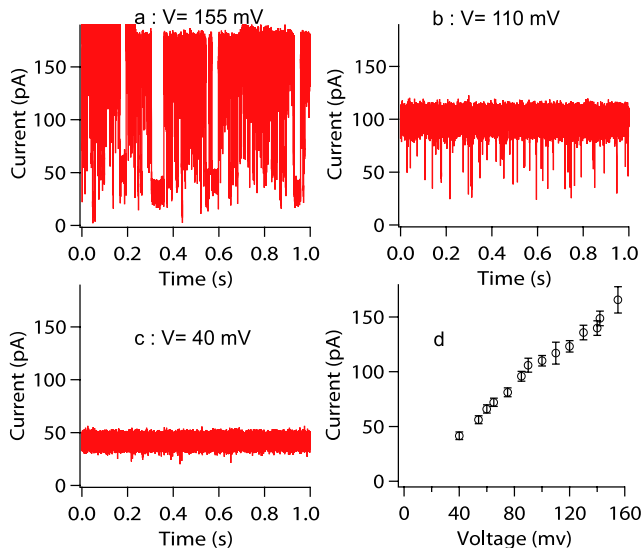

FIG. 1 (color online). Single-channel current traces through an α-hemolysin pore inserted into a planar lipid bilayer as a function of applied voltage V obtained by adding dextran sulfate at 0.5 mg/ml: (a) $V = 155$ mV, (b) $V = 110$ mV, (c) $V = 40$ mV. Current curve as a function of applied voltage (d). The conductance deduced from the slope is 1069 ± 15 pS.
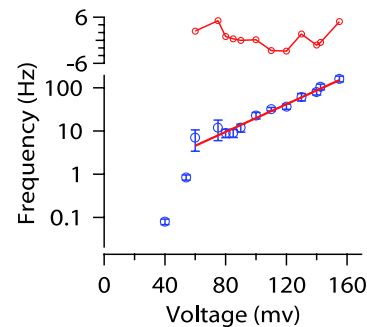

FIG. 2 (color online). Frequency of events versus applied voltage. Top: Linear scale. Bottom: Semilog scale. We do see two different regimes. The crossover occurs at $V = 60$ mV. The line between experimental points is an exponential fit: $f = f_0 \exp(V/V_0)$ with $f_0 = 0.5$ Hz and $V_0 = 27.2 \pm 0.29$ mV, with $V_0 = k_BT/ze$ and $k_BT/e = 25.7$ mV. The upper graph represents the deviation from the fit.
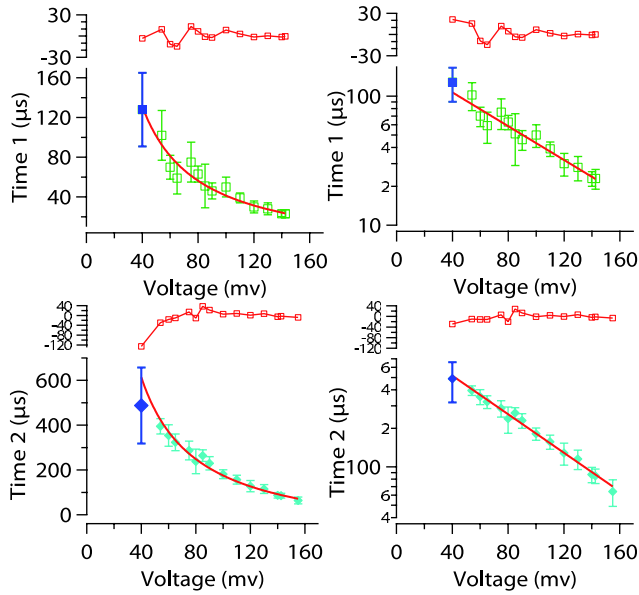
FIG. 3 (color online).   Duration of events versus applied voltage. Top: Short blockade time. Bottom: Long blockade time. Graphs on the left are on linear scale and those on the right on the semilog scale. The line is a fit of the equation $f(V) = (a/V) + b$ (left) or $f(V) = A \exp(V/V_c)$. We found for the short time $a = 5995 \pm 733\ \mu s\,mV$, $b = -18.6 \pm 6.5\ \mu s$ and $A = 195 \pm 33.5\ \mu s$, $V_c = 66 \pm 7.1$ mV. For the long time $a = 29\,240 \pm 1960\ \mu s\,mV$, $b = -117 \pm 17\ \mu s$ and $A = 1035 \pm 109\ \mu s$, $V_c = 58 \pm 3.6$ mV. The values at 40 mV are obtained by statistical analysis of the blockades along the current trace (10–50 events) but not with classical statistical analysis with a histogram of number of events as a function of T_t (> 1000 events). The upper graph represents the deviation from the fit.

the long time is clearly more convenient (Fig. 3). We have also performed experiments with a high molecular weight dextran sulfate 500 kg/mol (KCl 0.1M) (Fig. 4). The mean long blockade duration increases by a factor of 23, $\langle t_{8\ kDa} \rangle = 0.7 \pm 0.1$ ms and $\langle t_{500\ kDa} \rangle = 16 \pm 4$ ms, when the molecular weight of the polyelectrolyte increases by a factor of 62.5. Since the pore has a finite length and translocation is subject to large chain end effects, these data show that the polyelectrolyte is transported through the pore. We propose to associate the long blockades to the transport of the dextran sulfate chains through α-hemolysin and the short blockade to the phenomena of straddling of the chains at the pore entrance. Molecular dynamic simulations of DNA translocation show that the same level of blocking current is found if the polyelectrolyte is either straddling the pore or transported through the pore, but the blockade duration is longer for the translocation event [28,30]. Experiments performed on protein pores [1] or synthetic nanopores [29] have also shown that the short blockade duration corresponds to DNA chains interacting with the channel but failing to cross the pore and that the long blockades are consistent with the transport of polyelectrolyte through the pore. At all voltages, the population of short events is larger than that of long events.
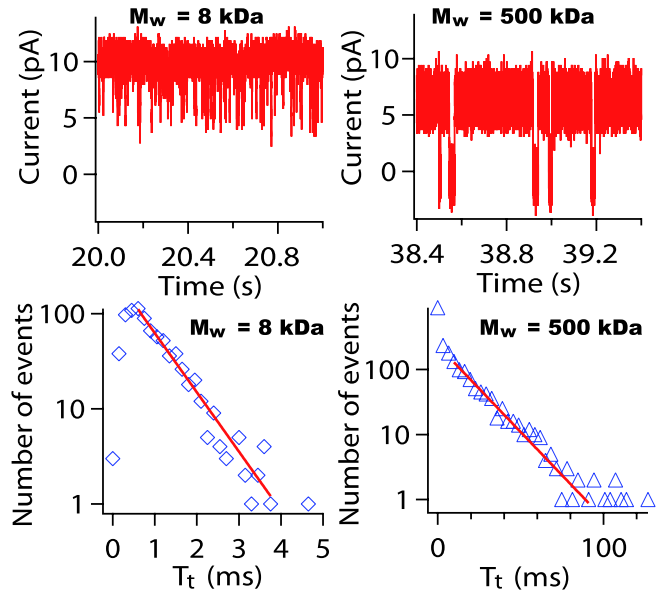

FIG. 4 (color online).   Single-channel current traces through a α-hemolysin pore inserted into a planar lipid bilayer obtained by adding either dextran sulfate 8 kDa or dextran sulfate 500 kDa at 0.5 mg/ml (upper panel). Distribution of blockade time T_t for different dextran sulfate molecular weight (lower panel). The dextran sulfate is added to the *cis* compartment in 0.1M KCl, pH = 7.4 buffer, at a final concentration of 0.5 mg/ml.

The limiting stage of the translocation process could thus be the search of suitable conformations for entering the pore but not the transport of the molecules through the channel [28].

We have estimated the effective charge of the polyelectrolyte inside the pore from the voltage dependence of the translocation time (Fig. 3), $V_c = 58 \pm 3.6$ and $z_{pore} = 0.44 \pm 0.03$. The effective charge is much lower than the one deduced from the charge density of the dextran sulfate chains using Manning theory. If the dielectric constant of pore environment is that of water, the global condensation of negative charges of dextran sulfate inside the channel is expected to be around 85%, yielding $z_{bulk} = 7.5$. With the experimental value $z = 0.44 \pm 0.03$, the global condensation is found to be much larger: around 99%. The low value of the effective charge observed experimentally could be associated with an increased condensation of the counterions due to the confinement of the charges in the medium of low dielectric constant [37]. In the theory of Zhang and Shklovskii [37], the effective charge of the chains in neutral pore is in practice related to the normalized ionic current $\langle I_B \rangle / \langle I_0 \rangle$, where $\langle I_0 \rangle$ is the ionic current in the empty pore and $\langle I_B \rangle$ the mean blockade current. This ratio contains all the free-energy factors associated with the electrostatic interactions, screening effects, and confinement of the electric field in the pore. It represents the effective section of the pore available for ionic motion. In the range of applied voltage and salt concentration explored, the normalized ionic current is constant (Fig. 5). We find, respectively, $\langle I_B \rangle / \langle I_0 \rangle = 0.23 \pm 0.04$ and
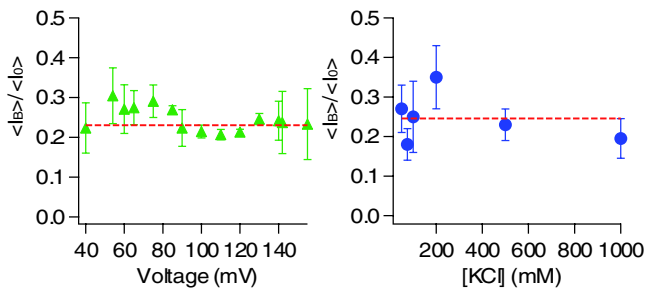
FIG. 5 (color online).   The normalized ionic current $\langle I_B \rangle / \langle I_0 \rangle$ as a function of applied voltage (left) or versus salt concentration KCl (right). The line corresponds to the average value $\langle I_B \rangle / \langle I_0 \rangle = b$, with $b = 0.24 \pm 0.04$ or $b = 0.24 \pm 0.02$, respectively, for the applied voltage or ionic strength dependence.

$\langle I_B \rangle / \langle I_0 \rangle = 0.24 \pm 0.02$. Under these conditions, electrical field or ionic strength do not influence the conduction process of ions inside the pore in the presence of a confined dextran sulfate chain. With single stranded DNA, the normalized ionic current is smaller, $\langle I_B \rangle / \langle I_0 \rangle = 0.09$ or 0.12, respectively, on DNA entry on either $3'$ or $5'$ side orientation [38], because the diameter of single strand chain (~ 1.4 nm) is higher than that of dextran sulfate (~ 0.4 nm). With DNA, the mean blockade current depends on ionic strength and voltage [39], and is probably due to the reduction of the cross section available for ion motion inside the pore.

We thank very much Boris Shklovskii for useful discussions. We are grateful to Jonathan James Ward for kindly correcting the language of the manuscript.

---

*Author to whom correspondence should be addressed.
Juan.pelta@bio.u-cergy.fr

[1] J. J. Kasianowicz, E. Brandin, D. Branton, and D. W. Deamer, Proc. Natl. Acad. Sci. U.S.A. **93**, 13 770 (1996).

[2] L. Song, M. R. Hobaugh, C. Shustak, S. Cheley, H. Bayley, and J. E. Gouaux, Science **274**, 1859 (1996).

[3] Y. Jung, H. Bayley, and L. Movileanu, J. Am. Chem. Soc. **128**, 15 332 (2006).

[4] S. M. Bezrukov and J. J. Kasianowicz, Eur. Biophys. J. **26**, 471 (1997).

[5] M. Pastoriza-Gallego, G. Oukhaled, J. Mathé, B. Thiébot, J. M. Betton, L. Auvray, and J. Pelta, FEBS Lett. **581**, 3371 (2007).

[6] M. Akeson, D. Branton, J. J. Kasianowicz, E. Brandin, and D. W. Deamer, Biophys. J. **77**, 3227 (1999).

[7] M. Bates, M. Burns, and A. Meller, Biophys. J. **84**, 2366 (2003).

[8] G. Oukhaled, J. Mathé, A. L. Biance, L. Bacri, J. M. Betton, D. Lairez, J. Pelta, and L. Auvray, Phys. Rev. Lett. **98**, 158101 (2007).

[9] H. Bayley and P. S. Cremer, Nature (London) **413**, 226 (2001).

[10] S. M. Bezrukov, I. Vodyanoy, R. A. Brutyan, and J. J. Kasianowicz, Macromolecules **29**, 8517 (1996).

[11] G. Oukhaled, C. Amiel, L. Bacri, E. Raphael, J. L. Sikorav, and L. L. Auvray, in *Proceedings of the 40th International Symposium on Macromolecules* [e-polymers E002, L1188 (2005)].

[12] R. J. Murphyand and M. Muthukumar, J. Chem. Phys. **126**, 051101 (2007).

[13] A. F. Sauer-Budge, J. A. Nyamwanda, D. K. Lubensky, and D. Branton, Phys. Rev. Lett. **90**, 238101 (2003).

[14] J. Mathé, J. H. Visram, V. Viasnoff, Y. Rabin, and A. Meller, Biophys. J. **87**, 3205 (2004).

[15] P. Hänggi, P. Talkner, and M. Borkovec, Rev. Mod. Phys. **62**, 251 (1990).

[16] W. Sung and P. J. Park, Phys. Rev. Lett. **77**, 783 (1996).

[17] E. Slonkina and A. B. Kolomeisky, J. Chem. Phys. **118**, 7112 (2003).

[18] Y. Kantor and M. Kardar, Phys. Rev. E **69**, 021806 (2004).

[19] D. Reguera, G. Scmid, P. S. Burada, J. M. Rubi, P. Reimann, and P. Hängi, Phys. Rev. Lett. **96**, 130603 (2006).

[20] O. Flomenbom and J. Klafter, Phys. Rev. E **68**, 041910 (2003).

[21] A. Meller, L. Nivon, and D. Branton, Phys. Rev. Lett. **86**, 3435 (2001).

[22] A. Storm, C. Storm, J. Chen, H. Zandbergen, J. F. Joanny, and C. Dekker, Nano Lett. **5**, 1193 (2005).

[23] A. Cacciuto and E. Luijten, Phys. Rev. Lett. **96**, 238104 (2006).

[24] S. Matysiak, A. Montesi, M. Pasquali, A. B. Kolomeisky, and C. Clementi, Phys. Rev. Lett. **96**, 118103 (2006).

[25] S. E. Henrickson, M. Misakian, B. Roberston, and J. J. Kasianowicz, Phys. Rev. Lett. **85**, 3057 (2000).

[26] A. Meller and D. Branton, Electrophoresis **23**, 2583 (2002).

[27] D. Fologea, J. Uplinger, B. Thomas, D. S. Mcnabband, and J. Li, Nano Lett. **5**, 1734 (2005).

[28] J. B. Heng, C. Ho, T. Kim, C. Timp, A. Aksimentiev, Y. V. Grinkova, S. Sligar, K. Shulten, and G. Timp, Biophys. J. **87**, 2905 (2004).

[29] A. Mara, S. Siwy, C. Trautmann, J. Wan, and F. Kamme, Nano Lett. **4**, 497 (2004).

[30] A. Aksimentiev, J. B. Heng, G. Timp, and K. Schulten, Biophys. J. **87**, 2086 (2004).

[31] I-C. Yeh and G. Hummer, Proc. Natl. Acad. Sci. U.S.A. **101**, 12 177 (2004).

[32] G. Menestrina, J. Membr. Biol. **90**, 177 (1986).

[33] See EPAPS Document No. E-PRLTAO-100-015816 for statistical analysis of a current trace. For more information on EPAPS, see http://www.aip.org/pubservs/epaps.html.

[34] G. Oukhaled, L. Bacri, J. Mathé, J. Pelta, and L. Auvray, "Effect of Screening on the Transport of Polyelectrolytes through Nanopores," Europhys. Lett. (to be published).

[35] P. G. De Gennes, Adv. Polym. Sci. **138**, 91 (1999).

[36] T. Ambjörnsson, S. P. Apell, Z. Konkoli, E. A. Di Marzio, and J. J. Kasianowicz, J. Chem. Phys. **117**, 4063 (2002).

[37] J. Zhang and B. I. Shklovskii, Phys. Rev. E **75**, 021906 (2007).

[38] J. Mathé, A. Aksimentiev, D. R. Nelson, K. Schulten, and A. Meller, Proc. Natl. Acad. Sci. U.S.A. **102**, 12 377 (2005).

[39] D. Jan Bonthuis, J. Zhang, B. Hornblower, J. Mathé, B. I. Shklovskii, and A. Meller, Phys. Rev. Lett. **97**, 128104 (2006).